Oxygen vacancy formation energy and its effect on spontaneous polarization in Bi$_4$Ti$_3$O$_{12}$: A first-principles theoretical study

T. Hashimoto[1] and H. Moriwake[2]

[1]*Research Institute for Computational Sciences (RICS), National Institute of Advanced Industrial Science and Technology (AIST), Tsukuba Central 2, 1-1-1 Umezono, Tsukuba, Ibaraki 305-8568, Japan*

[2]*Nanostructures Research Laboratory, Japan Fine Ceramics Center, 2-4-1 Mutsuno, Atsuta, Nagoya 456-8587, Japan*

We have studied the formation energy of oxygen vacancy and its effect on spontaneous polarizations of Bi$_4$Ti$_3$O$_{12}$ (BT) by first-principles theoretical calculations. We have found that neutral and +2 charged oxygen vacancies prefer sites in the Bi$_2$O$_2$ layers, while +1 charged oxygen vacancies are not stable. The spontaneous polarizations of the perfect-crystal BT in both a and c directions are in agreement with experiment. We have also shown that even if neutral or charged oxygen vacancies exist in a Bi$_2$O$_2$ layer, the spontaneous polarizations are not altered significantly from those of the perfect crystal.

I. INTRODUCTION

Ferroelectric random access memories (FeRAMs) are one of the nonvolatile memories and are beginning to be used in commercial products.[1] One of the problems in using FeRAM in actual device is that the polarization tends to decrease after many cycles of polarization reversal during device operation (fatigue). A possible cause of the fatigue is related to the oxygen vacancies,[2] and the role of the oxygen vacancy in ferroelectrics has been studied both experimentally and theoretically.[3–5] Among many ferroelectrics, those with the Aurivillius layer structure,[6] especially Bi$_4$Ti$_3$O$_{12}$ (BT) related compounds such as (Bi,La)$_4$Ti$_3$O$_{12}$,[7–13] have attracted considerable attention due to their fatigue endurance as well as their large remnant polarization, lead-free nature, and relatively low processing temperatures. As for the mechanism of the fatigue endurance of materials with the Aurivillius layer structure, it is suggested that oxygen vacancies prefer to stay in the Bi$_2$O$_2$ layers where their effect upon the polarization is thought to be small and not in the octahedral site that controls polarization.[2] Several studies have been done on the oxygen vacancy site in the Aurivillius layer structure. From x-ray photoemission spectroscopy (XPS) measurements for a BT ceramics, it was suggested that oxygen vacancies may be preferably present in the vicinity of the Bi ions in the Bi$_2$O$_2$ layers.[7] From other XPS measurements for BT films, it was suggested that oxygen vacancies may also exist in the perovskite layers.[8] A theoretical study using a shell model and treating only +2 charged oxygen vacancies for the ferroelectric phase of BT,[13] and a first-principles theoretical study treating only neutral oxygen vacancies for the high-temperature (>948 K) paraelectric phase of BT (Ref. 12) have shown that the oxygen vacancy formation energy is smallest in Bi$_2$O$_2$ layers.

In this Brief Report, we have calculated oxygen vacancy formation energy of the room-temperature ferroelectric phase of BT. We have dealt with not only neutral but also charged oxygen vacancies and have shown that the oxygen vacancy formation energy is the lowest in the Bi$_2$O$_2$ layer site for both neutral and charged vacancies, supporting previous theoretical studies. We have also calculated spontaneous polarization of BT using the Berry phase method.[14,15] For a perfect crystal, it is in agreement with the experiment although

it is slightly overestimated. In the case of the supercell containing one oxygen vacancy in the Bi$_2$O$_2$ layer, the spontaneous polarization is not affected significantly by oxygen vacancies.

II. METHOD

All calculations were done using a program package "STATE" (Simulation Tool for Atom TEchnology).[16,17] Our calculations are based on the density-functional theory (DFT) within a generalized gradient approximation (GGA) of Perdew *et al.*[18] Vanderbilt's ultrasoft pseudopotentials[19] are used for Ti 3p, 3d, and O 2p components, while other components are described by the Troullier-Martins norm-conserving pseudopotentials.[20] Wave functions are expanded in a plane-wave basis set, and the cut-off energies for wave functions and augmentation charges are 25 and 225 Ry, respectively.

In the case of the calculations using a primitive cell, we used four k points in the irreducible Brillouin zone. All the atomic coordinates were relaxed, while the conventional cell lattice constants were fixed to the experimental values of 5.4463, 5.4083, and 32.8329 Å in a, b, and c directions, respectively,[21] where a and c are directions of the larger and the smaller spontaneous polarizations, respectively [Figs. 1(c)–1(e)]. In the case of the calculations using a supercell with vacancies, we used a larger supercell of $2a \times 2b \times c$ (304 atoms for a perfect crystal) to avoid vacancy-vacancy interactions. Only the Γ point was used for the k-point sampling in the Brillouin zone, and all the atom coordinates were relaxed after introducing vacancies. The electronic contribution of the polarization was calculated using the Berry phase formalism.[14,15]

III. RESULTS

A. Energy

As for the space group for BT at low temperatures, although many experiments support monoclinic structures with space group $B1a1$,[22–25] the structural refinements fit well to orthorhombic structure with space group $B2eb$ (No. 41).[23] The two structures are very close to each other, and the largest difference between the two is rotations of Ti1O$_6$ octahedra around the c axis [Figs. 1(c)–1(h)]. In order to check the
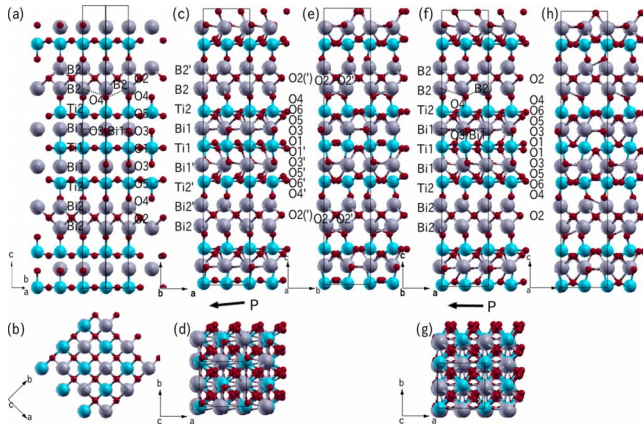
FIG. 1. (Color online) Side and top views of the atomic structure of [(a) and (b)] the paraelectric (space group $I4/mmm$), [(c)–(e)] ferroelectric (space-group $B1a1$), and [(f)–(h)] ferroelectric phases (space-group $B2eb$). Gray (large), blue (medium), and red (small) circles represent Bi, Ti, and O atoms, respectively. The solid line represents the primitive cell for (a) and (b) and conventional cell for (c)–(h). The arrows under (c) and (f) represent the directions of the spontaneous polarizations. In $I4/mmm$ and $B2eb$ models, definitions of atoms are the same as the $B1a1$ model except that $Xn'=Xn$ (X=Bi, Ti, O, and $n=1,2,\ldots$). In the $I4/mmm$ model, O6=O6'=O5.

stability of these two structures, with a fixed unit cell common to the two structures, we relaxed all atom coordinates assuming space group symmetries $B1a1$ (Ref. 22) and $B2eb$ (Ref. 23) and found that the former was more stable than the latter by 0.035 eV / 2 f.u. The tendency is the same for the full potential linearized augmented planewave (FLAPW) calculation by Cai *et al.*[26] and for the projector augmented wave (PAW) calculation by Shrinagar *et al.*[27] (0.06 eV / 2 f.u.) in which the atom positions and unit cell are both relaxed. Due to the similarity of the two structures, the calculated spontaneous polarizations for the two structures were also close: 0.602 C/m^2 (0 C/m^2) and 0.581 C/m^2 (0.064 C/m^2) in the a (c) direction for the $B2eb$ and $B1a1$ structure, respectively. In the present calculations, we used the $B1a1$ structure for all the calculations except for the Born effective charge calculations.

The calculated band gap for the perfect crystal is 2.27 eV, while from a LAPW calculation using GGA it is 2.57 eV,[26] which are smaller than 3.35 eV by optical transmission spectra of the single crystal of BT (Ref. 28) and 3.00 eV by optical transmission spectra of BT thin films.[29]

B. Vacancy formation energy

The supercell used for this calculation is shown in Figs. 1(c)–1(e) together with the definition of the independent atom sites. There are six and twelve independent oxygen atom sites for the $B2eb$ and $B1a1$ models, respectively. In the present study, because the two structures are similar and the computational cost including atom relaxation is heavy, we only calculated for six oxygen atoms On ($n=1,\ldots,6$) in the $B1a1$ model.

Oxygen vacancy formation energy is defined as

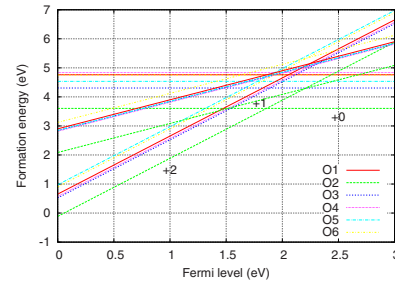$$F(D^q) = E(D^q) + q(\varepsilon_F + E_{\mathrm{VBM}}) - E(P) + (1/2)E(O_2),$$

FIG. 2. (Color online) Oxygen vacancy formation energies for charge states 0, +1, and +2. Each slope corresponds to the charge state q, and it is labeled for O2. The zero of Fermi energy is set to E_{VBM}. $E_{\mathrm{CBM}}=2.27$ eV in the present calculation.

where $E(P)$, $E(D^q)$, and $E(O_2)$ are the total energies corresponding to the perfect crystal, the supercell containing defect D in charge state q, and the O_2 molecule. ε_F is the Fermi energy measured from the valence-band maximum (VBM) E_{VBM}. In this calculation, the chemical potential for oxygen is half of the total energy of the spin polarized O_2 molecule, i.e., $\mu_O = \mu_O^{O_2} = 1/2E(O_2)$. This condition corresponds to the oxygen-rich limit. Although the chemical potentials of the constituent atoms μ_i are variables, in this study, we do not discuss μ_i dependency of the formation energy. If $\mu_O < \mu_O^{O_2}$, the formation energies shift rigidly downward and the vacancy formations become easier. Even in this case, the relative stability among V_{On}^q's are the same.

As seen in Fig. 2, the O2 site is the lowest oxygen vacancy formation energy site for BT for charge states 0, +1, and +2. The differences between $F(V_{O2}^q)$ and $F(V_{On}^q)$ for the next stable defect are 0.70, 0.73, and 0.64 eV for $q=0$, +1, and +2, respectively. +1 charge states were not stable for all vacancy sites. When ε_F is close to the VBM (p doped condition), the formation energy $F(V_{O2}^{2+})$ becomes negative, implying that V_{O2}^{2+} is easily formed in this condition. The result that V_{O2} is the most stable oxygen vacancy site is in agreement with the shell-model calculation by Snedden *et al.*[13] and also in agreement with the first-principles calculation for neutral oxygen vacancy in the high-temperature paraelectric phase by Noguchi *et al.*[12]

In the case of V_{O2}^{0+}, the vacancy state is within the band gap, which is occupied by two electrons, and the charge density of the vacancy state is concentrated on the vacancy site and on the neighboring Bi atoms [Fig. 3(a)]. The green arrows in the figure correspond to ten times of the atom relaxations from their original positions before relaxation to their positions after relaxation. The atoms with large relaxations are concentrated in the Bi_2O_2 layer. The average of the six Bi-Bi distances of the four Bi atoms neighboring the vacancy in the case of V_{O2}^{0+} (V_{O2}^{2+}) is 2% shorter (10% longer) than the corresponding value for the perfect crystal, implying that small inward (large outward) relaxations of neighboring atoms occur around V_{O2}^{0+} (V_{O2}^{2+}). This relaxation is relatively simple as compared to $PbTiO_3$,[4] in which oxygen vacancy prefers a site in the Ti-O$\cdots$Ti chain along the polarization direction and the neighboring Ti atoms move in the opposite directions to each other, creating opposite polarizations. Since the atom relaxations are concentrated in the Bi_2O_2 layer and the relaxation of atoms does not have an apparent
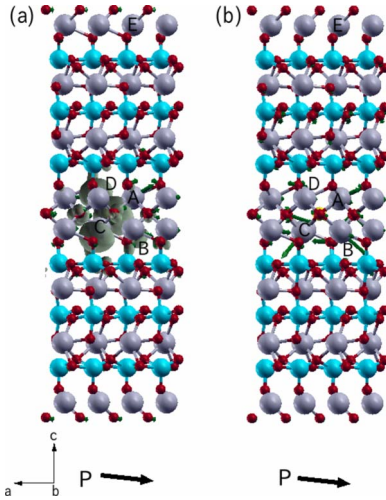
FIG. 3. (Color online) The relaxed atomic structure of the supercell containing (a) V_{O2}^{0+} and (b) V_{O2}^{2+}. The yellow circle in the center represents the vacancy site. The green arrows correspond to ten times of the atom relaxations from their original positions before relaxation to their positions after relaxation. The charge-density isosurface ($0.001/a.u.^3$) by the gray area corresponds to the vacancy state. The black arrows in the bottom of the figure represent the direction of the spontaneous polarization. A–E are Bi atoms whose Z^*'s are discussed in the text. B and D are blocked from view.

mechanism to disturb polarization unlike in PbTiO$_3$, it is expected that oxygen vacancies in BT do not significantly disturb dielectric polarization.

C. Polarization

The spontaneous electric polarization is expressed as[14,15]

$$\mathbf{P}_e^{(\lambda)} = (-ief/8\pi^3)\sum_{n=1}^{M}\int_{BZ} d\mathbf{k}\langle u_{n\mathbf{k}}^{(\lambda)}|\nabla_{\mathbf{k}}|u_{n\mathbf{k}}^{(\lambda)}\rangle,$$

where λ denotes the set of internal parameters of the crystal structure corresponding to the polarization path, $u_{n\mathbf{k}}$ is the periodic part of the Bloch wave function $\psi_{n\mathbf{k}}$, f is the occupation number of states in the valence band (in spin-degenerate system $f=2$), and M is the number of occupied bands. In practical calculations of the Berry phase, the wave functions are available only for a finite k-point mesh, and we use the discretized formula for the k-space integration. The k-point meshes for the perfect crystal are (8,3,1) and (4,2,4) for the calculation of $\mathbf{P}_e^{(\lambda)}$ in the $\mathbf{a}^*$ and $\mathbf{c}^*$ directions, respectively. The corresponding ones for the crystal containing V_{O2}^{0+} and V_{O2}^{2+} are (3,1,1) and (1,1,2) for $\mathbf{P}_e^{(\lambda)}$ in the $\mathbf{a}^*$ and $\mathbf{c}^*$ directions, respectively.

As a $\lambda=0$ structure, we used a high-temperature paraelectric phase structure of BT. In the case of the perfect crystal and V_{O2}^{0+} containing supercell, the systems are insulators for all λ's. In the case of the V_{O2}^{2+} containing supercell, although the system was not an insulator at $\lambda=0$, after relaxation of atoms keeping the paraelectric structure, it became an insulator.

1. Born effective charge

We have calculated Born effective charges (Z^*'s) of paraelectric and ferroelectric phases ($B2eb$ model) for BT

TABLE I. Born effective charge along the polarization direction for paraelectric and ferroelectric phase ($B2eb$ model). The difference with nominal ionic charge is shown in parentheses.

	Nominal	Para.	%	Ferro.	%
Bi1	3	5.90	(96.8)	4.72	(57.3)
Bi2	3	5.03	(67.6)	4.64	(54.7)
Ti1	4	7.44	(86.0)	6.07	(51.8)
Ti2	4	5.88	(47.1)	5.30	(32.5)
O1	−2	−4.32	(116.0)	−3.48	(74.0)
O2	−2	−3.04	(52.1)	−2.89	(44.5)
O3	−2	−3.29	(64.3)	−2.74	(37.0)
O4	−2	−2.13	(6.6)	−1.94	(−3.0)
O5	−2	−3.88	(93.9)	−3.58	(79.0)
O6	−2			−3.07	(53.5)
Sum		−0.001		0.02	

along the direction of spontaneous polarization by displacing each atom slightly and calculating the resulting change in the polarization by Berry phase method. The definition of atoms is shown in Fig. 1. The results are shown in Table I. The acoustic sum $\Sigma_I Z_I^*$ in our calculations were −0.001 and 0.02 for the paraelectric and ferroelectric phases, respectively. For both the paraelectric and ferroelectric phases, Z^*'s are much enhanced if they are compared to nominal ionic charges 3, 4, and −2 for Bi, Ti, and O, respectively, except for O4.

BT is composed of a perovskite-type Bi$_2$Ti$_3$O$_{10}$ unit and a Bi$_2$O$_2$ layer. In the perovskite-type Bi$_2$Ti$_3$O$_{10}$ unit, Z^*'s for Ti and O1, O5, and O6 are enhanced because when the Ti-O distance shortens a charge transfer from O to Ti occurs by changes in hybridization between O $2p$ and Ti $3d$ orbitals.[30–32]

It was shown that, although Z_A^*'s are close to their nominal ionic charge for many ABO$_3$ type perovskites, Z_{Pb}^*'s are enhanced.[31] In the case of BT, Z_{Bi1}^* is also enhanced. These large Z_A^*'s should also be due to the change in hybridization of Pb $6s$ or Bi $6s$ and $6p$ with O $2p$ (Refs. 26, 28, 33, and 34) when Pb-O or Bi-O bond lengths change. For atoms in the Bi$_2$O$_2$ layer, Z_{Bi2}^* and Z_{O2}^* are also enhanced due to the same reason.

O3 and O4 are displaced in the direction almost perpendicular to the Ti-O bond but in the direction of the neighboring Bi [Figs. 1(a) and 1(f)], and hence Z_{O3}^* is enhanced. However, Z_{O4}^* is close to its nominal ionic charge. This should be related to the difference of environment between O3 and O4, as discussed by Postnikov et al.:[35] O4 is bonded with only one Ti, terminating the chain of TiO$_6$ octahedra, and is separated from the Bi2 atom. The widths of the partial density of states for O4 $2s$ and $2p$ are narrower than other oxygen atoms, suggesting hybridization with Bi is suppressed.

We also note that the magnitude of Z^*'s for the ferroelectric phase is smaller than those for the paraelectric phase, like in other perovskites such as BaTiO$_3$.[30] Due to these large structure sensitivities of Z^*'s, it is difficult to correctly predict spontaneous polarization by using Z^*'s.[30] Instead, we have calculated it by changing the atom configuration parameter λ by small amounts.

TABLE II. Born effective charges along the *a* axis for four Bi atoms next to V_{O2}^{0+} and V_{O2}^{2+} and for Bi atom in another Bi_2O_2 layer that is separated from the vacancy (Fig. 3). The corresponding value for Bi in a perfect crystal (*B2eb* model) is 4.64, and the nominal ionic charge is 3.

	V_{O2}^{0+}	V_{O2}^{2+}
A	4.57	4.54
B	5.19	3.96
C	3.40	4.47
D	3.70	4.38
E	4.63	4.62

We have calculated Z^*'s along the *a* axis for four Bi atoms next to V_{O2}^{0+} and V_{O2}^{2+} (Fig. 3) and summarized them in Table II. Although they are enhanced compared to the nominal ionic charge, they have an overall tendency to be smaller than that in a perfect crystal and show site dependency due to asymmetric relaxation. Z^* for a Bi atom in another Bi_2O_2 layer (E in Fig. 3) that is separated from the vacancy is close to the perfect crystal value. The similar tendencies are also found for HfO_2.[36]

2. Spontaneous polarization

The spontaneous polarization of BT perfect crystal is 0.581 and 0.064 C/m^2 for the *a* and *c* directions, respectively. These values are in agreement with experimental values 0.50 ± 0.10 and 0.04 ± 0.001 C/m^2 for *a* and *c* directions, respectively.[37] The errors may be due to imperfection of the samples, which may lower the polarization. The errors also may be due to the temperature difference between the experiment (25 °C) and theory (0 K) since decreasing temperature away from the Curie temperature increases the value of the spontaneous polarization. The spontaneous polarization of BT containing one V_{O2}^{0+} (V_{O2}^{2+}) in the supercell was 0.614 and 0.051 C/m^2 (0.614 and 0.060 C/m^2) for the *a* and *c* directions, respectively. These values are very close to those for the perfect crystal. This result indicates that even if an isolated oxygen vacancy exists in BT, its effect on the spontaneous polarization should be very small.

IV. CONCLUSION

We have calculated oxygen vacancy formation energies of BT and have shown that for the ferroelectric phase it is smallest at the Bi_2O_2 site for neutral and +2 charged states. This result is in agreement with the suggestion by Scott *et al.* for $SrBi_2Ta_2O_9$, and reinforces the results by shell-model calculations for the ferroelectric phase and first-principles calculations for the paraelectric phase. We have also calculated spontaneous polarization of BT as a Berry phase of the wave functions obtained with first-principles calculations. The spontaneous polarizations were 0.58 and 0.06 C/m^2 in the *a* and *c* directions, respectively, which are in agreement with experiments. We have also shown that when an oxygen vacancy exists in the Bi_2O_2 layer, the atom relaxations are mainly concentrated in that layer and the spontaneous polarization is not altered significantly from that of the perfect crystal.

[1] J. F. Scott, Science **315**, 954 (2007).

[2] J. F. Scott and M. Dawber, Appl. Phys. Lett. **76**, 3801 (2000).

[3] Y. Kitanaka *et al.*, Appl. Phys. Lett. **90**, 202904 (2007).

[4] C. H. Park and D. J. Chadi, Phys. Rev. B **57**, R13961 (1998).

[5] L. He and D. Vanderbilt, Phys. Rev. B **68**, 134103 (2003).

[6] C. A. Paz de Araujo *et al.*, Nature (London) **374**, 627 (1995).

[7] C. Jovalekic *et al.*, Appl. Phys. Lett. **72**, 1051 (1998).

[8] B. H. Park *et al.*, Appl. Phys. Lett. **74**, 1907 (1999).

[9] B. H. Park *et al.*, Nature (London) **401**, 682 (1999).

[10] U. Chon *et al.*, Phys. Rev. Lett. **89**, 087601 (2002).

[11] Y. Noguchi *et al.*, Jpn. J. Appl. Phys., Part 2 **44**, L570 (2005).

[12] Y. Noguchi *et al.*, Jpn. J. Appl. Phys., Part 1 **44**, 6998 (2005).

[13] A. Snedden *et al.*, J. Solid State Chem. **177**, 3660 (2004).

[14] R. D. King-Smith and D. Vanderbilt, Phys. Rev. B **47**, 1651 (1993).

[15] D. Vanderbilt and R. D. King-Smith, Phys. Rev. B **48**, 4442 (1993).

[16] Y. Morikawa, Phys. Rev. B **63**, 033405 (2001).

[17] T. Hayashi *et al.*, J. Chem. Phys. **114**, 7615 (2001).

[18] J. P. Perdew *et al.*, Phys. Rev. Lett. **77**, 3865 (1996).

[19] D. Vanderbilt, Phys. Rev. B **41**, 7892 (1990).

[20] N. Troullier and J. L. Martins, Phys. Rev. B **43**, 1993 (1991).

[21] Y. Noguchi (private communication).

[22] A. D. Rae *et al.*, Acta Crystallogr., Sect. B: Struct. Sci. **46**, 474 (1990).

[23] C. H. Hervoches and P. Lightfoot, Chem. Mater. **11**, 3359 (1999).

[24] Y. Shimakawa *et al.*, Appl. Phys. Lett. **79**, 2791 (2001).

[25] Y. I. Kim and M. K. Jeon, Mater. Lett. **58**, 1889 (2004).

[26] M.-Q. Cai *et al.*, Chem. Phys. Lett. **401**, 405 (2005).

[27] A. Shrinagar *et al.*, Acta Crystallogr., Sect. A: Found. Crystallogr. **64**, 368 (2008).

[28] T. Goto *et al.*, Mater. Res. Bull. **40**, 1044 (2005).

[29] H. Gu *et al.*, Thin Solid Films **283**, 81 (1996).

[30] P. Ghosez *et al.*, Phys. Rev. B **58**, 6224 (1998).

[31] W. Zhong *et al.*, Phys. Rev. Lett. **72**, 3618 (1994).

[32] W. A. Harrison, *Electronic Structure and the Properties of Solids* (Dover, New York, 1980).

[33] R. E. Cohen, Nature (London) **358**, 136 (1992).

[34] J. Íñiguez *et al.*, Phys. Rev. B **67**, 224107 (2003).

[35] A. V. Postnikov *et al.*, Phys. Rev. B **52**, 11805 (1995).

[36] E. Cockayne, Phys. Rev. B **75**, 094103 (2007).

[37] S. E. Cummins and L. E. Cross, J. Appl. Phys. **39**, 2268 (1968).